VOL. 12, NO. 21, NOVEMBER 2017 ISSN 1819-6608
ARPN Journal of Engineering and Applied Sciences

www.arpnjournals.com

EVALUATING DAMAGE TO REINFORCED CONCRETE DURING MECHANICAL COMPRESSION AND BENDING TESTS

Denis D. Dann, Tatyana V. Fursa, Konstantin Yu. Osipov and Maxim V. Petrov
Institute of Non-Destructive Testing, National Research Tomsk Polytechnic University, Tomsk, Russia
E-Mail: mvp17@tpu.ru

ABSTRACT

The article proposes a method for evaluating damage to reinforced concrete subjected to uniaxial compression and four-point bending. The method is based on measuring and analyzing the parameters of electric and acoustic emissions and electric response to impact. It is established that the main signs marking the start of the cracking process are: the appearance of high-amplitude acoustic and electromagnetic emission signals changes in the spectral composition of the electrical signal, and the increased attenuation coefficient of the electric response's energy. Continuous or recurrent monitoring can be used to assess deterioration processes in reinforced concrete subjected to mechanical stress.

Keywords: Non-destructive testing, acoustic, electromagnetic emission, electric response to impact, reinforced concrete, mechanical testing.

1. INTRODUCTION

The wide use of reinforced concrete in important structures and buildings calls for strict requirements concerning its operational reliability. Polymer fiber reinforcement, which is resistant to corrosion and has a high strength-to-weight ratio as compared to conventional steel reinforcement, has recently gained high popularity along with traditional steel reinforcement [1]. Over time, cracks appear and develop in concrete, ultimately leading to unexpected structural failure. To ensure safe operation, it is necessary to have reliable information about the formation and evolution of cracks within the structure. To this end, many new concrete testing methods are being developed, including the acoustic and electromagnetic emission method [2-5], ultrasonic testing [6-7], nonlinear acoustic methods [8-9], impact echo methods [10-11], non-contact ultrasonic methods [12], methods based on detecting surface waves with laser [13], electrical tomography methods based on surface probing with conductive sensors [14] and the method based on impact-caused mechanoelectric transduction [15-21].

The essence of the mechanoelectric transduction method is that the object of research is exposed to elastic impact so that spherical acoustic waves start spreading within the concrete sample. The acoustic waves cause the displacement of the double electrical layers at the phase interface as well as the polarization of the piezoelectric quartz contained in the concrete's sand and gravel. This generates an alternating electric field, which is then detected by a signal receiver placed near the subject. A large number of sources of mechanoelectric transduction with different directions of the electric axes makes it possible to reliably reflect the changing parameters of elastic waves as they interact with various defects in the concrete sample and thus reveal the nature of these defects.

Deterioration processes in reinforced concrete structures can be identified via either continuous or recurrent monitoring. This article discusses a comprehensive approach to evaluating development of cracks based on measurement and analysis of electromagnetic and acoustic emissions and electric responses to impact in the process of uniaxial compression and four-point bending of reinforced concrete.

2. MATERIALS AND METHODS

2.1. Materials

Experimental studies were carried out using laboratory samples of reinforced concrete subjected to uniaxial compression and bending. For the uniaxial compression tests, samples of concrete with steel and fiberglass reinforcement were manufactured. The 100 × 100 × 100 mm samples were made of heavy concrete, in which one treaded steel or fiberglass reinforcing bar with a diameter of 10 mm and a length of 150 mm was placed during the concrete formation. The concrete samples were produced to the specifications of the Russian GOST Standard 7473-2010. For the bending tests, samples sized 100 × 100 × 400 mm were manufactured of the same heavy concrete, each containing a reinforcing cage of two steel or fiberglass reinforcing bars with diameters of 6 mm and 8 mm and a length of 400 mm, joined by crossbars.

2.2. Test methods

During compression and bending tests, simultaneous recording of electromagnetic and acoustic emissions and recurrent recording of electric responses to impact was carried out using custom software and hardware. The hardware system included a portable measuring probe, a power supply unit, an I/O card, and a notebook. The portable probe consisted of a metal cup housing the impact device and a differential sensor. Figure-1a shows the entire system, and Figure-1b – the measuring probe.

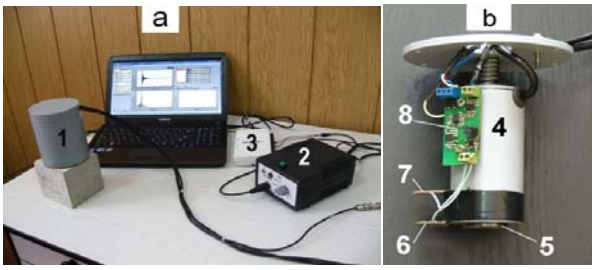

Figure-1. Photos of the measuring system (a) and the measuring probe (b) inside the metal cup. 1 - remote measuring probe, 2 - power supply, 3 - NI USB-6212 I/O card, 4 - impact device, 5 - metal plate, 6 - measuring electrode, 7 - compensation electrode, 8 - differential amplifier board.

Mechanical impacts were delivered via the electromechanical impact device (4), which was an electromagnet with graded impact force. In order to exclude local defects in the area of contact between the impacting body and the sample and the appearance of the elastic impact pulse, the impacts were carried out through a metal plate (5) mounted to the bottom cover of the impact device. The impact load used was around 100 N, and the duration of the impact pulse was 60 microseconds. A differential electric sensor was used to record the electrical signal, which ensured a significant increase in the signal-to-interference ratio. The receiver of the differential electrical sensor consisted of two receiving metal plates measuring 20 × 20 mm. One plate (6) was placed parallel to the sample surface at a distance of 2 mm and served as the measuring one. The second plate (7) was parallel to the first at a distance of 25 mm from the sample and served as the compensating one. The signal from the sensor was recorded using the NI USB-6212 multifunction I/O board, converting the electrical signal to digital form. Acoustic signals were measured using a standard Olympus V1011 piezo-transducer and the Olympus Panametrics 5058PR internal amplifier.

The IP-500 press machine was used in the uniaxial compression and bending tests. Compression tests were performed at a constant loading speed of 0.3 kN/s. Bending tests consisted of four-point bending with the loading speed of 0.05 kN/s. During the loading process, the load and displacement were recorded recurrently with 1 s intervals. The compression and bending measurements were carried out as follows. The measuring probe (1) was attached to the side surface of the sample with rubber bands. Then the concrete sample with the attached probe was placed either on the lower plate of the press (for the compression test) or on the roller bearings (for the bending test). The distance between the upper and lower bearings for the four-point bending tests was set according to the GOST 10180-2012 and ASTM C78/C78M standards, and loading was carried out until destruction of the sample. Electrical and acoustic signals are recorded during the loading process and sampling frequency was 100 kHz. In addition, the recurrent impacts were performed every 5-10 s.

3. EXPERIMENTAL RESULTS AND DISCUSSIONS

The parameters of acoustic and electromagnetic emissions and electric response to impact during compression and bending of reinforced concrete were examined using the above method with the objective of identifying and validating the diagnostic criteria for evaluation of cracking processes.

3.1. Analysis of elastoplastic characteristics of reinforced concrete during compression and bending

Using the method described above, the nature of the transformation of the elastoplastic characteristics of concrete with different reinforcement types subjected to the compression and bending tests was studied (Figure-2).

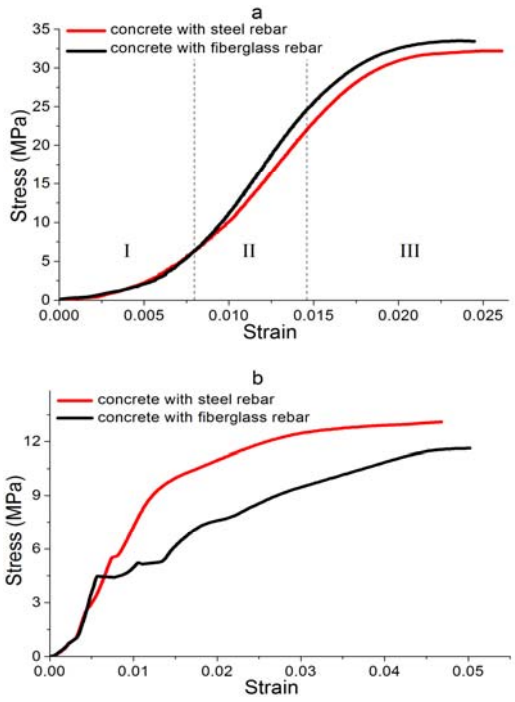

Figure-2. Stress-strain curves during compression (a) and bending (b) of concrete samples reinforced with steel and fiberglass.

Stress-strain curves at a constant compression loading speed (Figure-2a) have three distinct sections representing three stages of the process. The Figure shows break down into the stages of load curve for the concrete reinforced by fiberglass rebar.

The first section (I) is nonlinear and associated with the compaction of the sample's surface layer, which has a lower hardness. The second section (II) is linear – well approximated by a straight line – and represents the stage of quasi-elastic deformation. The third section (III) is sharply nonlinear and associated with the appearance and spread of cracks. The concrete samples with different types of reinforcement subjected to uniaxial compression show no significant differences in the mechanical and

elastoplastic characteristics: the variations in strength and elastic modulus do not exceed 10%.

As can be seen from Figure-2b, the maximum bending load the samples with steel reinforcement withstand is higher compared to the ones with plastic reinforcement. The appearance and spread of cracks during bending is accompanied by a jump in deformation while the load remains the same. Since plastic reinforcement has smaller elastic modulus of elasticity, its deformation extent is much greater and the segments of the curve representing the appearance of individual cracks are more distinct for the same load values.

3.2. Acoustic and electromagnetic emissions

The appearance and development of cracks under mechanical stress generates acoustic and electromagnetic emissions [2-5]. These emissions were recorded during the uniaxial compression and four-point bending tests. Figure-3 shows typical relationships of acoustic and electromagnetic emissions from reinforced concrete subjected to uniaxial compression and four-point bending.

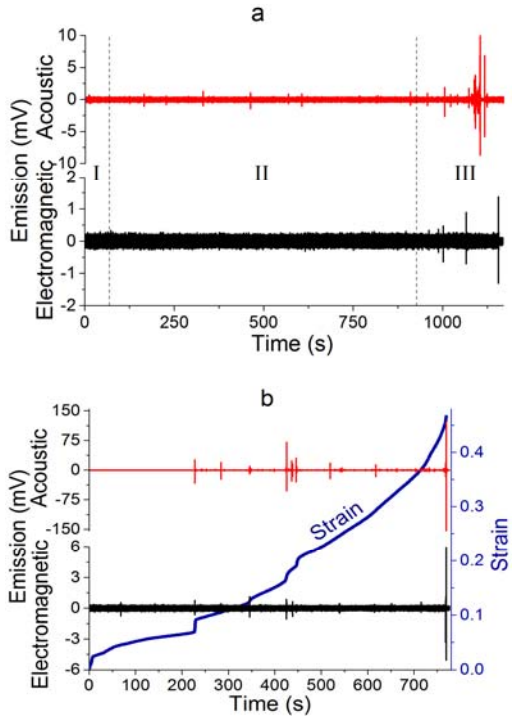

Figure-3. Changes in acoustic and electromagnetic emissions from concrete with fiberglass (a) and steel (b) reinforcement during loading (I, II, III represents three stages of the compression process).

The results of the tests show that the efficiency of electromagnetic emission is lower than that of acoustic emission. From the analysis of the experimental data shown in Figure-3a, it follows that the transition of concrete past the yield point is accompanied by the appearance of acoustic and electromagnetic emission signals that exceed the noise level by a factor of 2 or greater. As Figure-3b shows, high-amplitude acoustic and electromagnetic emission signals occur at the time of appearance and uneven spread of cracks under bending stress. The characteristics of samples with steel reinforcement behave similarly.

3.3. Analysis of the electrical signal spectra

Mechanical stresses caused by external load lead to the development of cracks in the concrete. With an increase in the external mechanical load, the size and concentration of cracks in the strained area increases in comparison with the undisturbed area of the sample. The front of the acoustic wave travels across these areas, which leads to its distortion. These distortions of the acoustic wave must be reflected in the characteristics of the electric response, which is in turn interconnected with the elastic waves. When in the process of traveling through the concrete sample acoustic waves encounter cracks, they are partly reflected from the cracks and partly propagate around the cracks. With multiple passage of the acoustic wavefront through the sample, oscillations of different periods develop in the defective sample. The spectral characteristic of the signal obtained using Fourier transform monitors the presence of oscillations with different periods. Figure-4 shows a two-dimensional image of the changes in the normalized spectral density of the power of electrical signal in fiberglass-reinforced concrete subjected to uniaxial compression and four-point bending.

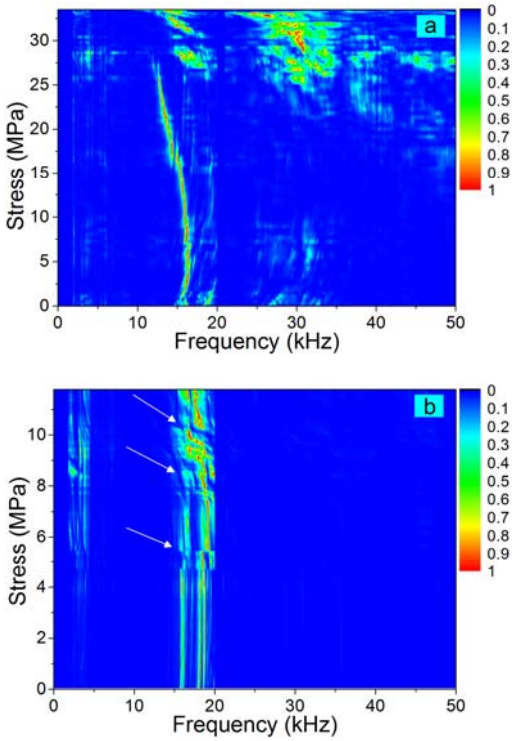

Figure-4. Normalized spectral density of the power of electrical signal power during uniaxial compression (a) and bending (b) of concrete with fiberglass reinforcement.

At the initial moment of loading, the spectrum of the electrical signal from the fiberglass-reinforced concrete (Figure-4a) has a fairly simple structure with a dominant maximum at 15.5 kHz and less significant components within 29-32 kHz. Upon the transition to the cracking area (at loads above 25 MPa), there is a significant broadening of the spectrum with no pronounced peak and a large number of practically equivalent spectral components. In contrast to that, upon bending of the concrete sample (Figure-4b) the signal spectrum changes less significantly. At the moment of appearance of cracks, an uneven shift of the dominant spectral peak is observed, represented on the normalized power spectral density chart as slanted gaps. In Figure-4b, these gaps are marked by arrows. The differences in the variation of the signal spectra during compression and bending are associated with the differences in the nature of deterioration.

Figure-5 shows the fractured samples after compression and bending tests.

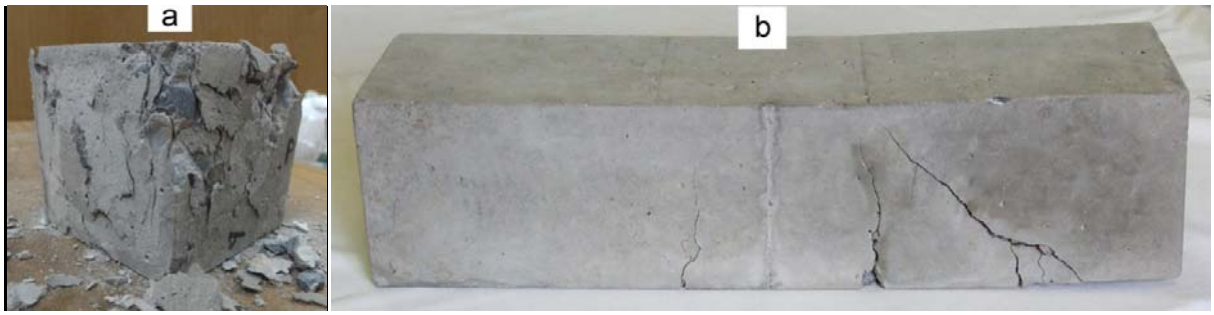

Figure-5. Photographs of the fractured samples subjected to compression (a) and bending (b).

As shown in Figure-5, a large number of cracks were formed during compression throughout the entire body of the sample, while during bending only a few cracks developed. Consequently, during compression more significant changes in the spectrum of electric responses occur as compared to bending.

3.4. Attenuation of the electric responses' energy

The formation of cracks in concrete subjected to uniaxial compression and bending leads to a change in the characteristics of the wave processes that develop in the samples due to mechanical impact. Scattering of elastic waves on cracks reflects the process of fading with time. The frequency-time analysis was used to determine the attenuation coefficient of the signal's energy [12, 17].

This technique allows tracking the attenuation of the energy of the response as the function of time in any selected range of frequencies.

The processing of the experimental data was performed with custom software developed in LabVIEW. In the program, the size of the sliding window is selected, and the pitch for the window shift depending on the time signal realization is set. The frequency range to be analysed is selected in the energy spectrum of the signal with a cursor. The total energy of the response spectrum for each window in the selected frequency range is calculated.

In this particular case, the frequency range from 1 to 40 kHz was chosen for the analysis. This frequency range contains the main part of the energy of the electric responses appearing in the concrete samples under elastic shock excitation. The size of the sliding window was 300 μs, and consistent shifting of this window depending on time was done with the spacing of 30 μs. A detailed technique to determine the attenuation coefficient of the electric response energy is presented in [16, 22].

Figure-6 shows the relationship between the attenuation coefficient of the signal's energy and the external compression load.

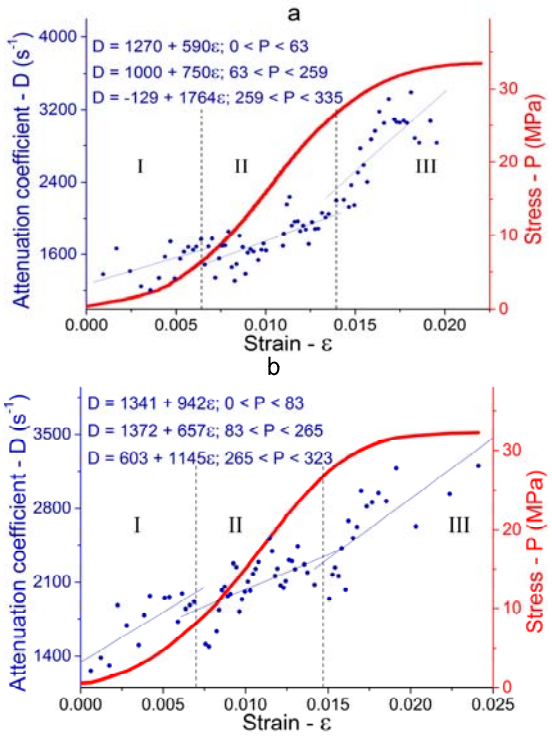

Figure-6. Changes in the attenuation coefficient of the electric responses' energy depending on the value of the external compression load when compressing concrete with fiberglass (a) and steel (b) reinforcement.

In the process of compression of concrete samples, an increase in the attenuation coefficient of the electric responses' energy is observed throughout all three stages of the curve. In order to identify consistent patterns of the changes in the analyzed parameters and their behavior during different loading stages, an approximation of the experimental results was performed using piecewise linear functions (shown in the graphs). Upon the transition to the crack appearance stage, an increase in the proportionality coefficient in the approximating lines is observed in comparison to the quasi-elastic deformation stage. This indicates a more significant signal attenuation at the cracking stage.

4. CONCLUSIONS

The changes patterns in the parameters of acoustic and electromagnetic emissions and electric responses to the impact in reinforced concrete subjected to uniaxial compression and four-point bending were examined. The studies were carried out using samples of heavy concrete with steel and fiberglass reinforcement.

Upon the transition to the fracture stage the following effects were observed:

- the appearance of acoustic and electromagnetic emission signals exceeding the noise level by a factor of 2 or greater;
- significant broadening of the signal spectrum during compression and uneven shift of the dominant spectral peak during bending;
- an increase in the attenuation coefficient of the electric responses' energy by a factor of 3 or greater. It was shown that the nature of the changes in the attenuation coefficient does not differ significantly for samples with different types of reinforcement.

Thus, the combination of the diagnostic features examined makes it possible to evaluate deterioration processes in concrete under mechanical stress. According to the results of the experiments, continuous and periodic monitoring may be used to detect the beginning of cracking processes. The results obtained can be used for estimation of the remaining service life of reinforced concrete structures.

ACKNOWLEDGEMENTS

This study has been funded with a Russian Science Foundation Grant (Project No. 16-19-10119).

REFERENCES

[1] Pendhari S.S., Kant T. and Desai Y.M. 2008. Application of polymer composites in civil construction: A general review. Composite Structures. 84(2): 114-124.

[2] Aggelis D.G., Mpalaskas A.C. and Matikas T.E. 2013. Investigation of different fracture modes in cement-based materials by acoustic emission. Cement and Concrete Research. 48: 1-8.

[3] Kyriazopoulos A., Anastasiadis C., Triantis D. and Brown C.J. 2011. Non-destructive evaluation of cement-based materials from pressure-stimulated electrical emission Preliminary results. Construction and Building Materials. 25(4): 1980-1990.

[4] Koktavy P. 2009. Experimental study of electromagnetic emission signals generated by crack generation in composite materials. Measurement Science Technology. 20(1): 15704.

[5] Triantis D., Stavrakas I., Kyriazopoulos A., Hloupis, G. and Agioutantis Z. 2012. Pressure stimulated electrical emissions from cement mortar used as failure predictors. International Journal of Fracture. 175: 53-61.

[6] Molero M., Aparicio S., Al-Assadi G., Casati M.J., Hernández M.G. and Anaya J.J. 2012. Evaluation of freeze–thaw damage in concrete by ultrasonic imaging. NDT & E International. 52: 86-94.

[7] Iyer S., Sinha S.K., Pedrick, M.K. and Tittmann B.R. 2012. Evaluation of ultrasonic inspection and imaging systems for concrete pipes. Automation in Construction. 22: 149-164.

[8] Bui D., Kodjo S.A., Rivard P. and Fournier B. 2013. Evaluation of Concrete Distributed Cracks by Ultrasonic Travel Time Shift under an External Mechanical Perturbation: Study of Indirect and Semi-direct Transmission Configurations. Journal of Nondestructive Evaluation. 32: 25-36.

[9] Antonaci P., Bruno C., Gliozzi A. and Scalerandi M. 2010. Monitoring evolution of compressive damage in concrete with linear and nonlinear ultrasonic methods. Cement and Concrete Research. 40(7): 1106-1113.

[10] Krzemień K. and Hager I. 2015. Post-fire assessment of mechanical properties of concrete with the use of the impact-echo method. Construction and Building Materials. 96: 155-163.

[11] Liu P.-L. and Yeh P.-L. 2011. Spectral tomography of concrete structures based on impact echo depth spectra. NDT & E International. 44(8): 692-702.

[12] Tsai Y.T. and Zhu J. 2012. Simulation and Experiments of Airborne Zero-Group-Velocity Lamb Waves in Concrete Plate. Journal of Nondestructive Evaluation. 31: 373-382.

[13] Algernon D., Gräfe B., Mielentz F., Köhler B. and Schubert F. 2008. Imaging of the Elastic Wave Propagation in Concrete Using Scanning Techniques: Application for Impact-Echo and Ultrasonic Echo Methods. Journal of Nondestructive Evaluation. 27: 83-97.

[14] Smyl D., Rashetnia R., Seppänen A. and Pour-Ghaz M. 2017. Can Electrical Resistance Tomography be used for imaging unsaturated moisture flow in cement-based materials with discrete cracks? Cement and Concrete Research. 91: 61-72.

[15] Fursa T.V., Savelev A.V. and Osipov K.Yu. 2003. Interrelation between Electromagnetic Response Parameters and Impact Excitation Characteristics in Insulators. Technical Physics Journal. 48(11): 1419-1424.

[16] Osipov K.Yu. and Fursa T.V. 2013. Evaluating the Depth of Open Cracks in Concrete from Parameters of Electric Response to Elastic Impact Excitation. Technical Physics Letters. 39(5): 481-483.

[17] Fursa T.V., Dann D.D., Petrov M.V. and Korzenok I.N. 2016. Effect of Cyclic Freezing–Thawing on the Parameters of Electric Response to Elastic Shock Excitation of Reinforced Concrete. Russian Journal of Nondestructive Testing. 52(8): 463-468.

[18] Fursa T.V., Surzhikov A.P. and Dann D.D. 2010. Development of the technique of nondestructive testing of heterogeneous dielectric materials based on utilization of the mechanoelectric transformation phenomenon. Russian Journal of Nondestructive Testing. 46(1): 5-9.

[19] Fursa T.V., Utsyn G.E., Dann D.D. and Petrov M.V. 2017. Development Prospects for Nondestructive Testing of Heterogeneous Nonmetallic Materials by the Parameters of Electrical Response to a Shock Action. Russian Journal of Nondestructive Testing. 53(2): 104-110.

[20] Fursa T.V., Dann D.D., Petrov M.V. and Lykov A.E. 2017. Evaluation of Damage in Concrete under Uniaxial Compression by Measuring Electric Response to Mechanical Impact. Journal of Nondestructive Evaluation. 36(2): 30.

[21] Fursa T.V. 2010. Mechanoelectric Transformation in Cement-Sand Composites in the Course of Crack Formation Caused by Freezing-Thawing Cycles. Technical Physics Letters. 36(4): 348-350.

[22] Quiviger A., Payan C., Chaix J.-F., Garnier V. and Salin J. 2012. Effect of the presence and size of a real macro-crack on diffuse ultrasound in concrete. NDT & E International. 45: 128-132.